Forward-Speed Effects on Hydrodynamic Forces Acting on a Submerged Cylinder in Waves

Kashiwagi, Masashi
Research Institute for Applied Mechanics, Kyushu University : Associate Professor

VARYANI, Kamlesh
Department of Naval Architecture, Kyushu University : Graduate student

Ohkusu, Makoto
Research Institute for Applied Mechanics, Kyushu University : Professor

https://doi.org/10.5109/6781044

出版情報：Reports of Research Institute for Applied Mechanics. 34 (102), pp.1-26, 1987-09. 九州大学応用力学研究所
バージョン：

Reports of Research Institute for Applied Mechanics
Vol. XXXIV, No. 102, 1987

Forward-Speed Effects on Hydrodynamic Forces Acting on a Submerged Cylinder in Waves

By Masashi KASHIWAGI*, Kamlesh VARYANI† and Makoto OHKUSU‡

Two-dimensional radiation and diffraction problems are studied of a submerged circular cylinder moving with forward speed while oscillating under the effects of incident waves. After a linear formulation of the boundary-value problem, the numerical solution is obtained by solving the integral equation for the velocity potential on the body surface. With attention focused on the effects of forward speed on hydrodynamic forces, added mass, damping, wave-exciting force, resultant motions, and added resistance are computed. The speed-dependent terms in the body boundary condition, arising from the interactions between steady and oscillatory flow fields, are found to exert a considerable influence on the hydrodynamic forces.

The added resistance of a circular cylinder is approximately zero in head waves, whereas in following waves it becomes positive for $U/C < 1/2$ and negative for $1/2 < U/C < 1$ (where U is the body speed, C the phase velocity of incident wave). It is also shown by numerical computations that there is no added resistance if a circular cylinder is allowed to respond to the first-order hydrodynamic forces. We discussed the method of pressure calculation on the body surface on the premise that the principle of energy conservation must by satisfied in an inviscid fluid.

key words: Forward-speed effects, Circular cylinder, Radiation problem, Diffraction problem, Added resistance

1. Introduction

Since ships generally move with forward velocity while undergoing oscillatory motions in waves, the presence of forward speed should be taken into account in the calculations of hydrodynamic forces on and resultant motions of ships. However, even with present powerful computers, it is not so easy to solve

* Associate Professor, Research Institute for Applied Mechanics, Kyushu University.
† Graduate student, Department of Naval Architecture, Kyushu University.
‡ Professor, Research Institute for Applied Mechanics, Kyushu University.

a fully three-dimensional problem with the effects of forward speed consistently included. In the past three decades, the so-called strip theory was developed as an approximation for the three-dimensional ship-motion problem and has undergone a number of refinements. In a conventional strip theory, the forward-speed effects on the hull boundary condition are approximately taken into account, but the speed-dependent terms in the free-surface condition are neglected.

Ogilvie and Tuck[1)] presented a systematic perturbation procedure of examining the approximations involved in the strip theory and obtained some contributions to the cross-coupling coefficients in addition to the conventional results. These additional contributions, represented by some integral terms over the free surface, were calculated by Faltinsen[2)] and confirmed to give an improvement over the predictions of conventional strip theory. Since these additional contributions are essentially due to the term linearly proportional to the forward speed in the free-surface condition, the employment of the complete free-surface condition may provide more improvement.

Chapman[3)] initiated a drastically different approach to accomodate the forward-speed effects on the free-surface condition. The flow at each cross-section along the ship is analyzed in a quasi-two-dimensional manner, with interactions propagated downstream by the free-surface condition. The validity of this method was supported by the impressive agreement between calculations and experiments for the sway and yaw response of a flat plate. In such a quasi-three-dimensional method, only the effects of divergent waves are taken into account. The characteristics of genuine three-dimensional waves are rather intricate because of the combined effects of forward motion and sinusoidal oscillation of a body. However the calculations including all of the three-dimensional wave characteristics will be helpful for a proper understanding of the forward-speed effects.

Chang[4)] and Kobayashi[5)] obtained the direct numerical solution of a fully three-dimensional problem by using a source-distribution method. The results show good agreement with experiments and give an improvement over the strip-theory predictions. Since such numerical results contain the effects of three-dimensional interactions among the cross-sections of a ship as well as the effects of free surface, it is not easy to understand the role played by the forward-speed terms in the free-surface condition.

In the present paper, in order to obtain a physical understanding of the forward-speed effects on hydrodynamic forces acting on a body, a linearized two-dimensional problem is considered, where a long cylindrical body moves in the direction normal to its axis and oscillates sinusoidally in head or following waves. The free-surface condition used in this paper is the same as in the three-dimensional problem and hence the waves generated can be expected to contain essentially the same characteristics as those of three-dimensional waves. As will be shown later, in the two-dimensional problem four waves of different wavenumbers are generated. Thus, with information on the characteristics of individual waves, the forward-speed effects on hydrodynamic forces may be investigated in detail. The two-dimensional study presented here was initially started for a surface-piercing body. However, as in the steady translation problem discussed by Ursell[6], the unsteady problem seems to have a difficulty on the nonuniqueness of the solution, which is conceivably due to the singularities at the intersections of body and free surfaces. In fact, the numerical solution for the surface-piercing problem turned out not to satisfy the principle of energy conservation. Before discussing this problem further, we decided to study the problem for a submerged body, because the submerged-body problem is well-posed and thus there can be no problem of the kind stated above.

Recently, with an integral equation method, Grue and Palm[7] solved exactly the radiation and diffraction problems of a submerged circular cylinder oscillating in a uniform current and examined the properties of radiated and diffracted waves. Grue[8] also computed the time-periodic pressure loading, added mass, damping, and exciting forces on a submerged circular cylinder in a current. The present paper deals with almost the same problem as Grue did, but by putting emphasis on the investigation of the forward-speed effects, we will discuss other aspects related to the two-dimensional unsteady problem with forward velocity.

Under a linear assumption, the boundary conditions to be satisfied by the velocity potential are stated in Section 2. To obtain a solution, the integral equation for the velocity potential on the body surface is introduced in Section 3 together with the Green function satisfying appropriate boundary conditions. In Section 4, after defining the Kochin function and deriving the expression for the elevation of radiated waves at infinity, the characteristics of speed-dependent unsteady waves are summarized. In Section 5 the formulae are given for calculating the first-order hydrodynamic forces (added-mass and damping coefficients, wave-exciting forces) and for calculating the second-order steady force (added resistance). The contributions of steady perturbation potential to the body boundary condition are taken into account. These contributions result from the interaction between steady and oscillatory flow fields and thus represent the forward-speed effects on the body boundary condition, which are in this paper referred to as the m-vector contributions. With regard to the exciting force, the forward-speed version of the Haskind-Newman relation is derived. Numerical results and discussion are presented in Section 6. By comparing the two kinds of calculations including and excluding the m-vector contributions, the effects of forward speed arising from body and free surface conditions are separately examined. We discussed the method of pressure calculation on the body surface on the premise that the principle of energy conservation must be satisfied; that is, the damping force obtained by the pressure integral must be equal to the one evaluated from the amplitudes of outgoing waves at infinity. The motions of a circular cylinder responding to the first-ordr radiation and diffraction forces are calculated. With the effects of these motions taken into account, computations of the added resistance are also made. Numerical results presented in this paper have quite good accuracy, since the principle of energy conservation, the Timman-Newman relation[9] for the coupling coefficients, and the Haskind-Newman relation[10] in the diffraction problem are all satisfied with numerical errors less than 0.5%.

2. Boundary Value Problem

We consider a circular cylinder which is submerged under a free surface with its center placed at depth d. The cylinder is assumed to translate with constant forward velocity U and to oscillate sinusoidally with frequency ω.

As shown in Fig. 1, we define a Cartesian coordinate system moving with the

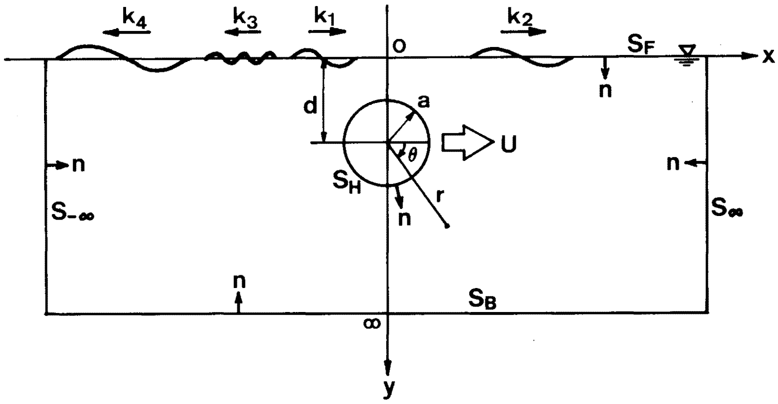

Fig. 1 Coordinate system and schematic representation of radiated waves.

same speed as the body, where the x-axis is positive in the direction of the body's forward motion and the y-axis positive downwards with $y=0$ taken as the mean position of the free surface. The fluid domain has infinite depth and horizontal extent and the fluid is assumed ideal with irrotational motion. Then a velocity potential can be introduced to describe the boundary-value problem, which is governed by the Laplace equation of the form

$$\left(\frac{\partial^2}{\partial x^2}+\frac{\partial^2}{\partial y^2}\right)\Phi(x, y\,;t)=0\ . \tag{1}$$

We decompose this velocity potential as follows

$$\Phi(x, y\,;t)=U\{-x+\varphi_s(x, y)\}+Re\{\phi(x, y)e^{i\omega t}\}\ . \tag{2}$$

Where $\varphi_s(x, y)$ is the steady-state perturbation potential due to the forward motion of the body and the second term in the right-hand side of Eq.(2) represents the unsteady velocity potential. Since the unsteady motions are assumed sinusoidal in time, the time dependence can be factored out as in Eq. (2). Then "unsteady" potential $\phi(x, y)$, which is to be solved, will be given in complex form. *Re* denotes that the final answer can be obtained by taking the real part of the product of $\phi(x, y)$ and the oscillatory time-dependence $e^{i\omega t}$. If the amplitude of incident wave is small in comparison to the wavelength, the resulting unsteady motions of a body and thus the unsteady potential ϕ can be all assumed small. Then the boundary conditions on the body and free surfaces can be linearized by neglecting second-order terms in ϕ. With the principle of linear superposition, we express the unsteady potential in the form

$$\phi(x, y) = \frac{gA}{i\omega_0}\{\varphi_I(x, y) + \varphi_D(x, y)\} + \sum_{j=1}^{2} i\omega\xi_j a\psi_j(x, y) \ . \tag{3}$$

Where $\varphi_I(x, y)$ and $\varphi_D(x, y)$ are respectively the incident-wave and diffraction potentials; these are normalized in terms of the amplitude A and the frequency ω_0 of incident wave. $\psi_j(x, y)$ is the radiation potential due to the j-th mode of body motion, nondimensionalized with the amplitude of motion ξ_j and the radius a of a circular cylinder, where j is the mode index, $j = 1$ for surge and $j = 2$ for heave. Since no disturbance is expected by the roll motion of a circular cylinder, the roll motion is not considered here.

By taking account of the contributions of steady perturbation potential, Timman & Newman[9] derived the linearized boundary condition on the body surface for the unsteady potential, which can be summarized as follows:

1) for radiation potential

$$\frac{\partial\psi_j}{\partial n} = n_j + \frac{U}{i\omega a} m_j \quad (j = 1, 2) \ , \tag{4}$$

where

$$\left.\begin{aligned} m_1\boldsymbol{i} + m_2\boldsymbol{j} &= -(\boldsymbol{n}\cdot\nabla)\boldsymbol{V} \ , \\ \boldsymbol{V} &= \nabla\{-x + \varphi_s(x, y)\} \ , \\ \boldsymbol{n} &= n_1\boldsymbol{i} + n_2\boldsymbol{j} \ . \end{aligned}\right\} \tag{5}$$

2) for diffraction potential

$$\frac{\partial\varphi_D}{\partial n} = -\frac{\partial\varphi_I}{\partial n} \ , \tag{6}$$

where

$$\varphi_I = e^{-ky \pm ikx} \ , \quad k = \omega_0^2/g \ . \tag{7}$$

Here n_j in Eq. (4) denotes the component of unit normal directed into the fluid and the second term in Eq. (4) represents the forward-speed effects, accounting for the interaction between the steady and oscillatory flow fields. The positive sign in the exponential function in Eq. (7) is taken for the incident wave propagating in the negative x-direction when seen from the moving reference frame. Conversely, the negative sign is for the wave propagating in the positive x-direction.

The free-surface boundary condition for the unsteady potential becomes more involved compared to the body boundary condition, if the contributions of steady perturbation potential are consistently retained. However in the present problem, since the body is submerged, the steady disturbances on the free surface may be small compared to the ones in the vicinity of the body surface. With this reason, we ignore the perturbation of the steady flow due to a submerged body and use the conventional free-surface condition given in the following form

$$\left[\left(i\omega-U\frac{\partial}{\partial x}\right)^2-g\frac{\partial}{\partial y}+\mu\left(i\omega-U\frac{\partial}{\partial x}\right)\right]\phi(x,y)=0\ ,\qquad \text{on } y=0\ . \tag{8}$$

Where the radiation condition at infinity has been imposed by including an artificial Rayleigh viscosity μ. Unless the bottom condition is imposed, the boundary-value problem is not completed. For the case of infinite depth, this condition is stated as

$$\nabla\phi\rightarrow 0\ ,\quad \text{as } y\rightarrow +\infty\ . \tag{9}$$

3. Integral Equation and Green Function

In order to obtain a solution satisfying the boundary conditions stated in the preceding section, the integral equation method is adopted. Applying Green's theorem in a fluid domain bounded by the surfaces shown in Fig. 1, we get

$$\phi(P)=-\int_S\left[\frac{\partial\phi(Q)}{\partial n}-\phi(Q)\frac{\partial}{\partial n}\right]G(P,Q)dl\ , \tag{10}$$

where

$$S=S_F+S_H+S_\infty+S_{-\infty}+S_B\ .$$

Here $P=(x,y)$ is the field point and $Q=(\xi,\eta)$ the source point. $G=(P,Q)$ denotes the Green function satisfying the free-surface condition, the radiation condition, and the condition of vanishing motion at $y=\infty$; these conditions are identical to the ones to be satisfied by ϕ. Taking account of these boundary conditions for G and ϕ, we can show that the expression (10) satisfies all of the boundary conditions except that on the body surface. If the field point P is situated on the body surface, the left-hand side of Eq. (10) is multiplied by 1/2. Thus we get the following equation

$$\frac{1}{2}\phi(P)-\int_{S_H}\phi(Q)\frac{\partial}{\partial n}G(P,Q)dl=-\int_{S_H}\frac{\partial\phi(Q)}{\partial n}G(P,Q)dl\ . \tag{11}$$

The normal derivative $\partial\phi/\partial n$ on the right-hand side is known from the body-boundary condition, so that Eq. (11) is the integral equation for the unknown velocity potential; this can be solved by direct numerical calculations.

The Green function $G(P,Q)$ for the present problem may be derived by the Fourier transform technique. The result is written in the form

$$G(x, y\,;\,\xi, \eta) = -\frac{1}{2\pi}\left[\ln\frac{r}{r_1} + \hat{G}(x-\xi, y+\eta)\right] , \tag{12}$$

where

$$\hat{G}(x, y) = -\int_{-\infty}^{\infty} \frac{e^{-|k|y-ikx}}{|k| - \frac{1}{g}(kU+\omega-i\mu)^2} dk$$

$$= \frac{K_0}{k_1-k_2}\{S_1(x, y) - S_2(x, y)\} + \frac{K_0}{k_3-k_4}\{S_3(x, y) - S_4(x, y)\} \tag{13}$$

$$S_j(x, y) = \int_0^{\infty} \frac{e^{-ky-ikx}}{k-k_j \mp i\mu} dk \ , \quad \text{for } j = \binom{1}{2} \ . \tag{14}$$

$$S_j(x, y) = \int_0^{\infty} \frac{e^{-ky+ikx}}{k-k_j + i\mu} dk \ , \quad \text{for } j = 3, 4 \ , \tag{15}$$

$$\left.\begin{matrix} k_1 \\ k_2 \end{matrix}\right\} = \frac{K_0}{2}[1-2\tau \pm \sqrt{1-4\tau}] \ , \quad \left.\begin{matrix} k_3 \\ k_4 \end{matrix}\right\} = \frac{K_0}{2}[1+2\tau \pm \sqrt{1+4\tau}] \ , \tag{16}$$

$$K_0 = \frac{g}{U^2} \ , \quad \tau = \frac{U\omega}{g} \ , \quad \left.\begin{matrix} r \\ r_1 \end{matrix}\right\} = \sqrt{(x-\xi)^2 + (y \mp \eta)^2} \ .$$

The integrals in Eqs. (14) and (15) can be transformed into alternative forms in terms of contour integrals in the complex k-plane. Since μ is a small positive quantity, the contour of integration is deformed to pass above (for $j = 1$) or below (for $j = 2, 3, 4$) the pole at $k = k_j$. With this information and the residue theorem, it is relatively easy to show that

$$S_j(x, y) = e^{-k_j z}\{E_1(-k_j z) \pm 2\pi i u(\mp Im.k_j z) u(1-2\tau)\} \ ,$$
$$\text{for } j = \binom{1}{2} \ , \tag{17}$$

$$S_j(x, y) = e^{-k_j \bar{z}}\ \{E_1(-k_j \bar{z}) - 2\pi i u(-x)\} \ , \quad \text{for } j = 3, 4 \ , \tag{18}$$

where

$$z = y + ix \ , \quad \bar{z} = y - ix \ .$$

Here $u(x)$ is Heaviside's unit function and $E_1(z)$ is the exponential integral of complex argument, defined by

$$E_1(z) = \int_z^{\infty} \frac{e^{-t}}{t} dt \quad arg\, z < \pi \ . \tag{19}$$

4. Wave Characteristics and Kochin Function

In order to examine the characteristics of radiated waves, let us first consider the behavior of the Green function at infinity; in this limit, with the asymptotic approximation of the exponential integral, it can be shown that the

Green function has the asymptotic form of

$$G(x, y\,;\,\xi, \eta) \sim -i\frac{u(1-4\tau)}{\sqrt{1-4\tau}}\left[e^{-k_1\zeta}u(\xi-x)+e^{-k_2\zeta}u(x-\xi)\right]$$
$$+i\frac{1}{\sqrt{1+4\tau}}\left[e^{-k_3\bar{\zeta}}\; u(\xi-x)-e^{-k_4\bar{\zeta}}\; u(\xi-x)\right] , \quad (20)$$

where

$$\zeta = y+\eta+i(x-\xi) \ , \quad \bar{\zeta} = (y+\eta)-i(x-\xi) \ .$$

Substituting this expression into Eq. (10) gives the asymptotic form of the velocity potential

$$\left.\begin{aligned}
&\phi(x, y) \sim i\frac{u(1-4\tau)}{\sqrt{1-4\tau}}H^{+}(k_2)e^{-k_2y-ik_2x} \ , \quad \text{as } x \to +\infty \ , \\
&\phi(x, y) \sim i\frac{u(1-4\tau)}{\sqrt{1-4\tau}}H^{+}(k_1)e^{-k_1y-ik_1x} \\
&\qquad +\frac{i}{\sqrt{1+4\tau}}\left[-H^{-}(k_3)e^{-k_3y+ik_3x}+ H^{-}(k_4)e^{-k_4y+ik_4x}\right] \ , \\
&\qquad\qquad \text{as } x \to -\infty
\end{aligned}\right\} \quad (21)$$

Here $H^{\pm}(k_j)$, $j = 1, 2, 3, 4$, is referred to as the Kochin function and defined by the following equations

$$\left.\begin{aligned}
H^{+}(k_j) &= \int_{S_H}\left[\frac{\partial\phi}{\partial n}-\phi\frac{\partial}{\partial n}\right]e^{-k_j\eta+ik_j\xi}dl \ , \quad \text{for } j = 1, 2 \ , \\
H^{-}(k_j) &= \int_{S_H}\left[\frac{\partial\phi}{\partial n}-\phi\frac{\partial}{\partial n}\right]e^{-k_j\eta-ik_j\xi}dl \ , \quad \text{for } j = 3, 4 \ .
\end{aligned}\right\} \quad (22)$$

In accordance with the decomposition of the velocity potential in Eq. (3), the Kochin function can be expressed in the form

$$\begin{aligned}
H^{\pm}(k) &= \frac{gA}{i\omega_0}H_D^{\pm}(k)+\sum_{j=1}^{2} i\omega\xi_j a H_j^{\pm}(k) \\
&= \frac{gA}{i\omega_0}\left\{H_D^{\pm}(k)-\sum_{j=1}^{2}\frac{\omega\omega_0 a}{g}\cdot\frac{\xi_j}{A}H_j^{\pm}(k)\right\} \equiv \frac{gA}{i\omega_0}H_F^{\pm}(k) \ , \quad (23)
\end{aligned}$$

where $H_D^{\pm}(k)$ and $H_j^{\pm}(k)$ are the nondimensionalized Kochin functions associated with the diffraction and radiation problems, respectively.

Using Eq. (21) and taking account of the equations for the phase velocity given by

$$\left.\begin{aligned}
C &= \sqrt{\frac{g}{k_j}} = \frac{\omega}{k_j}+U \ , &&\text{for } j = 1, 2 \ , \\
C &= \sqrt{\frac{g}{k_j}} = \mp\left(\frac{\omega}{k_j}-U\right) \ , &&\text{for } j = \binom{3}{4} \ ,
\end{aligned}\right\} \quad (24)$$

we obtain the elevation of two-dimensional radiated wave at infinity, in the form

$$\zeta_W(x) = \frac{1}{g}\Big(i\omega - U\frac{\partial}{\partial x}\Big)\phi(x,0)$$
$$\sim \begin{cases} A_2 e^{-ik_2x}\,, & \text{as } x \to \infty\,, \\ A_1 e^{-ik_1x} + A_3 e^{ik_3x} + A_4 e^{ik_4x}\,, & \text{as } x \to -\infty\,, \end{cases} \tag{25}$$

where

$$A_j = \begin{cases} -\sqrt{\dfrac{k_j}{g}}\dfrac{H^+(k_j)}{\sqrt{1-4\tau}}u(1-4\tau) & (j=1,2) \\ -\sqrt{\dfrac{k_j}{g}}\dfrac{H^-(k_j)}{\sqrt{1+4\tau}} & (j=3,4)\,. \end{cases} \tag{26}$$

From the above equations, it can be seen that for $\tau < 1/4$ an oscillating and translating body generates four waves of wavenumbers k_j $(j = 1, 2, 3, 4)$. To be more specific, at $x = \infty$ there exists k_2-wave radiating upstream, and at $x = -\infty$ k_1-wave propagating in the positive x-direction together with k_3- and k_4-waves radiating downstream. For $\tau > 1/4$, k_1- and k_2-waves are not generated and thus there exist only two downstream waves with wavenumbers k_3 and k_4.

These characteristics of radiated waves may be understood more easily by

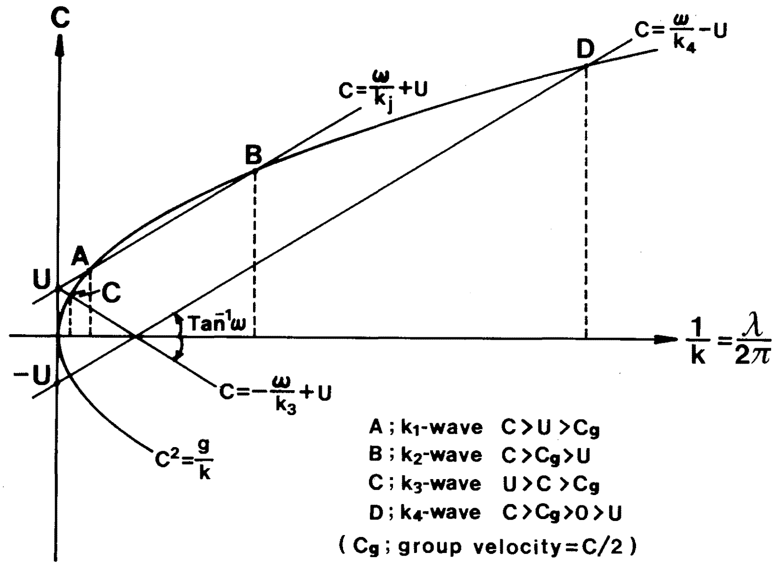

Fig. 2 Relations among body speed (U), phase velocity (C), and group velocity (C_g).

referring to Fig. 2. Fig. 2 shows the relation of the phase velocity C and the wavenumber k, in which the parabola represents the dispersion relation given by

$$C^2 = \frac{g}{k} , \tag{27}$$

and the straight lines represent the relations expressed by Eq. (24). The four wavenumbers, k_1, k_2, k_3, and k_4 are given as the solutions at cross points of parabola and straight lines. Note that the wave energy propagates with the group velocity and that, for infinite depth, the group velocity is half of the phase velocity. Schematically the group velocity is given as the ordinate at the intersection of the vertical axis and a tangent to the parabola. With these taken into account, the relations among phase velocity, group velocity, and body speed for individual waves may be found with ease. The results are shown also in Fig. 2. From these relations the propagating directions of k_j-waves ($j = 1, 2, 3, 4$) can be understood, which are shown schematically in Fig. 1 together with individual wavelengths.

It is confirmed from Fig. 2 or Eq. (16) that in the steady case $\omega = 0$, k_2 and k_4 vanish, while both k_1 and k_3 are equal to $K_0 = g/U^2$. Therefore it can be said that k_1- and k_3-waves originate from the steady forward-speed problem. On the other hand, in the limit of $U \to 0$, $\omega \neq 0$, both k_2 and k_4 are equal to $k = \omega_0^2/g$, but k_1 and k_3 tend to infinity. Thus k_2- and k_4-waves are considered to originate from the zero-speed problem. It should be noted that in the range of $\tau > 1/4$ k_1 and k_2 become complex and that for $\tau < 1/2$ the second term in braces in Eq. (17) has a contribution. Therefore, in the range of $1/4 < \tau < 1/2$ there can be waves propagating as well as decaying exponentially in the immediate vicinity of the body.

In the diffraction problem, besides the frequency of encounter ω, the frequency of incident wave ω_0 is introduced. The incident-wave frequency ω_0, which is defined in the space-fixed reference frame, is related to the wavenumber k by the dispersion relation of the form

$$\omega_0 = \sqrt{gk} . \tag{28}$$

Substituting this relation into Eq. (24), the expressions for the encounter frequency ω are given as follows

$$\left.\begin{aligned}
\omega &= \omega_0 - \frac{\omega_0^2}{g} U , && \text{for } k_1\text{-, } k_2\text{-waves} , \\
\omega &= \frac{\omega_0^2}{g} U - \omega_0 , && \text{for } k_3\text{-wave} , \\
\omega &= \omega_0 + \frac{\omega_0^2}{g} U , && \text{for } k_4\text{-wave} .
\end{aligned}\right\} \tag{29}$$

From these equations, it is obvious that there are three types of following waves depending on the forward velocity of the body, whereas the head wave is only the k_4-wave irrespective of the forward speed. In following waves, when the body speed is less than the group velocity, i. e. $U/C < 1/2$, the wavenumber of incident wave is equal to k_2. For the body speed greater than the group velocity but less than the phase velocity $1/2 < U/C < 1$, the incident wave is the k_1-wave, and for the body speed higher than the phase velocity $U/C > 1$, the k_3-wave.

5. Hydrodynamic Forces

We consider the unsteady component of the hydrodynamic pressure force, with the usual assumption that the oscillatory motions of the body and fluid are small. Using the expression (2) and neglecting second-order terms, the linearized hydrodynamic pressure is expressed in the form

$$p(x, y) = -\rho\left\{(i\omega + U\boldsymbol{V}\cdot\nabla)\phi + \frac{U^2}{2}(\boldsymbol{\alpha}\cdot\nabla)\,\boldsymbol{V}^2\right\}\ , \tag{30}$$

where

$$\boldsymbol{\alpha} = \xi_1\boldsymbol{i} + \xi_2\boldsymbol{j}\ .$$

The last term in Eq. (30) gives a force proportional to the unsteady displacement of the body, and hence an additional buoyancy force to the hydrostatic restoring force.

5.1. Added mass and damping

Since we are concerned with the unsteady pressure force associated with the added mass and damping, we will use Eq. (30) without the last term. Then, the unsteady hydrodynamic pressure force can be expressed as

$$F_i = -\int_{S_H} p(x, y)n_i dl = \sum_{j=1}^{2} T_{ij}\xi_j \qquad (i = 1, 2)\ , \tag{31}$$

where

$$T_{ij} = \rho a\int_{S_H}[i\omega + U\boldsymbol{V}\cdot\nabla]i\omega\psi_j(x, y)n_i dl \tag{32}$$

$$\equiv -(i\omega)^2\{A_{ij} + B_{ij}/i\omega\}\ . \tag{33}$$

Here A_{ij} and B_{ij} are respectively the added-mass and damping coefficients associated with the force in the i-th direction due to the j-th mode of motion. In Eq. (32), the term proportional to the steady velocity vector $\boldsymbol{V}$ can be transformed by means of Tuck's theorem[1)]

$$\int_{S_H}(\boldsymbol{V}\cdot\nabla)\psi_j n_i dl = -\int_{S_H}\psi_j m_i dl\ . \tag{34}$$

In view of the body boundary condition (4) for the radiation potential, we devide the unsteady potential ψ_j into two parts, in the form

$$\psi_j(x, y) = \varphi_j(x, y) + \frac{U}{i\omega a}\hat{\varphi}_j(x, y)\ . \tag{35}$$

Here, from Eq. (4), the potentials φ_j and $\widehat{\varphi}_j$ must satisfy the body boundary conditions of the form

$$\frac{\partial \varphi_j}{\partial n} = n_j \ , \quad \frac{\partial \widehat{\varphi}_j}{\partial n} = m_j \ . \tag{36}$$

Substituting Eqs. (34) and (35) into Eq. (32) and taking into account that the potentials φ_j and $\widehat{\varphi}_j$ are in general given in complex form, we get the expressions for the added-mass and damping coefficients

$$\frac{A_{ij}}{\rho a^2} = -\int_0^{2\pi} \varphi_{jc} n_i d\theta$$
$$-\left\{\frac{U}{\omega a}\int_0^{2\pi}[\widehat{\varphi}_{js}n_i - \varphi_{js}m_i]d\theta + \left(\frac{U}{\omega a}\right)^2 \int_0^{2\pi} \widehat{\varphi}_{jc} m_i d\theta\right\} , \tag{37}$$

$$\frac{B_{ij}}{\rho a^2 \omega} = \int_0^{2\pi} \varphi_{js} n_i d\theta$$
$$-\left\{\frac{U}{\omega a}\int_0^{2\pi}[\widehat{\varphi}_{jc}n_i - \varphi_{jc}m_i]d\theta - \left(\frac{U}{\omega a}\right)^2 \int_0^{2\pi} \widehat{\varphi}_{js} m_i d\theta\right\} , \tag{38}$$

where following notations have been used:

$$\left.\begin{aligned} &\varphi_j = \varphi_{jc} + i\varphi_{js} \ , \quad \widehat{\varphi}_j = \widehat{\varphi}_{jc} + i\widehat{\varphi}_{js} \ , \\ &dl = a d\theta \ . \end{aligned}\right\} \tag{39}$$

It is noteworthy that the first line of Eqs. (37) and (38) includes no forward-speed effects on the body boundary condition and the second line represents the forward-speed effects associated with the m-vector.

The damping coefficients B_{ij} can be associated with the work done to oscillate the body. This work should be equal to the energy flux of outgoing radiated waves under the assumption of an inviscid fluid. Based on this principle, Grue & Palm[7] derived an equation for calculating the damping force. An alternative derivation, applying an appropriate limiting operation on the three-dimensional result, is shown in Appendix A. The result is expressed in the form

$$\frac{B_{jj}}{\rho a^2 \omega} = \frac{1}{2}\left[\frac{|H_j^+(k_1)|^2 + |H_j^+(k_2)|^2}{\sqrt{1-4\tau}} + \frac{-|H_j^-(k_3)|^2 + |H_j^-(k_4)|^2}{\sqrt{1+4\tau}}\right] . \tag{40}$$

It should be emphasized that the value of Eq. (40) must coincide with the value calculated from Eq. (38).

If the perturbation of the steady flow is neglected, from Eq. (5) $\boldsymbol{V} = -\boldsymbol{i}$ and m_j $(j = 1, 2)$ becomes zero. Then, from Eq. (36), the potential $\widehat{\varphi}_j$ has no contribution. Therefore the second line on the right-hand side of Eqs. (37) and (38) is identically zero; this is equivalent to that the pressure on the body surface must be of the form

$$p(x, y) = -\rho i \omega \phi(x, y) \ . \tag{41}$$

However, if the approximation $\boldsymbol{V} = -\boldsymbol{i}$ is substituted in Eq. (30), the following result, which is customarily used in a linear ship-motion theory, can be obtained

$$p(x, y) = -\rho\left(i\omega - U\frac{\partial}{\partial x}\right)\phi(x, y) . \tag{42}$$

Apparently this differs from Eq. (41), and if Eq. (42) was integrated over the body surface, the second term of (42) would have nonzero contributions. Comparison of the damping coefficient obtained by Eq. (40) with the corresponding value by the pressure integration would tell us which is the correct expression, Eq. (41) or Eq. (42), for the pressure on the body surface. In conclusion, numerical results which will be presented later support Eq. (41), not the conventional expression.

5.2. Exciting forces

The exciting forces, acting upon the body restrained in its steady-state equailibrium position, can be calculated by substituting the sum of incident-wave and diffraction potentials into Eq. (30) as the unsteady potential ϕ and by integrating it over the body surface. We write the exciting force in the j-th direction obtained in such a manner, as follows

$$\begin{aligned} E_j &= \frac{\rho g A}{i\omega_0}\int_{S_H}(i\omega + UV\cdot\nabla)\{\varphi_I(x, y) + \varphi_D(x, y)\}n_j dl \\ &= \rho g A a\frac{\omega}{\omega_0}\int_0^{2\pi}\left(n_j - \frac{U}{i\omega a}m_j\right)\{\varphi_I + \varphi_D\}d\theta . \end{aligned} \tag{43}$$

There exists a relation known as the Haskind-Newman relation which gives the exciting forces with the Kochin function of the radiation problem, without having to solve the diffraction problem. Following Newman[10], we rederive this relation here with the present notations. First we note that the factor $(n_j - Um_j/i\omega a)$ appearing in Eq. (43) is the same as the right-hand side of Eq. (4) except for the sign of uniform velocity U. Thus, if we consider the reverse-flow radiation problem where the body is moving in the negative x-direction at the same speed U, the velocity potential of this reverse-flow problem, denoted by $\tilde{\phi}_j(x, y)$, satisfies the following boundary condition

$$\frac{\partial\tilde{\phi}_j}{\partial n} = n_j - \frac{U}{i\omega a}m_j , \quad \text{for } j = 1, 2 . \tag{44}$$

With this boundary condition, Eq. (43) can be written as

$$\frac{E_j}{\rho g A a} = \frac{\omega}{\omega_0}\int_0^{2\pi}(\varphi_I + \varphi_D)\frac{\partial\tilde{\phi}_j}{\partial n}d\theta . \tag{45}$$

By utilizing Green's theorem and then the boundary condition (6) for the diffraction problem, the following equation can be obtained

$$\int_0^{2\pi}\varphi_D\frac{\partial\tilde{\phi}_j}{\partial n}d\theta = \int_0^{2\pi}\tilde{\phi}_j\frac{\partial\varphi_D}{\partial n}d\theta = -\int_0^{2\pi}\tilde{\phi}_j\frac{\partial\varphi_I}{\partial n}d\theta . \tag{46}$$

Substituting this in Eq. (45), we get the Haskind-Newman relation in the form

$$\frac{E_j}{\rho g A a}=\frac{\omega}{\omega_0}\int_0^{2\pi}\left(\frac{\partial\tilde{\phi}_j}{\partial n}-\tilde{\phi}_j\frac{\partial}{\partial n}\right)\varphi_I d\theta$$
$$=\frac{\omega}{\omega_0}\tilde{H}_j^{\pm}(k)\ . \tag{47}$$

Where $\tilde{H}_j^{\pm}(k)$ denotes the Kochin function for the reverse-flow radiation problem, and the last form of Eq. (47) followed from Eq. (7) and the definition of the Kochin function given by Eq. (22).

Strictly, Eq. (44) is not correct for the body with no longitudinal symmetry, since the steady disturbance and hence the m-vector of the reverse-flow problem differ from those of the original problem. Of course, if the body is symmetrical about $x=0$, Eq. (47) follows exactly and $\tilde{H}_j^{\pm}(k)$ is related to the Kochin function of the original radiation problem in the form

$$\tilde{H}_j^{\pm}(k)=(-1)^j H_j^{\mp}(k)\ . \tag{48}$$

By comparison of the result of pressure integration, Eq. (43), with the Haskind-Newman formula, Eq. (47), we can check numerical accuracy of the solution for the diffraction problem.

5.3. Added resistance

The added resistance is the second-order steady force, but of practical interest to naval architects and ocean engineers. Grue & Palm[7] studied the mean second-order force on a circular cylinder. This force is the added resistance considered here, provided the signs in their analyses are reversed. The formulae derived by Grue & Palm are limited in a sense, since their derivation took account of the fact that a circular cylinder generates only two diffraction waves. In the present study, the added resistance not only of a restrained cylinder but also of a freely oscillating cylinder will be calculated. Therefore it is necessary to give the general expression for the added resistance.

With the principle of momentum conservation, the following equations can be obtained. (An alternative derivation from three-dimensional Maruo's formula[11] is presented in Appendix A.)

1) for incoming k_4-wave (head wave)

$$\frac{R_{AW}}{\frac{1}{2}\rho g A^2}=\frac{1}{2}\left[\frac{|H_D^+(k_1)|^2}{\sqrt{1-4\tau}}\left(1+\frac{k_1}{k_4}\right)+\frac{|H_D^+(k_2)|^2}{\sqrt{1-4\tau}}\left(1+\frac{k_2}{k_4}\right)\right.$$
$$\left.+\frac{|H_D^-(k_3)|^2}{\sqrt{1+4\tau}}\left(\frac{k_3}{k_4}-1\right)\right] \tag{49}$$

2) for incoming k_2-wave (following wave)

$$\frac{R_{AW}}{\frac{1}{2}\rho g A^2}=\frac{1}{2}\left[\frac{|H_D^+(k_1)|^2}{\sqrt{1-4\tau}}\left(\frac{k_1}{k_2}-1\right)+\frac{|H_D^-(k_3)|^2}{\sqrt{1+4\tau}}\left(1+\frac{k_3}{k_2}\right)\right.$$

$$-\frac{|H_D^-(k_4)|^2}{\sqrt{1+4\tau}}\left(1+\frac{k_4}{k_2}\right)] \tag{50}$$

3) for incoming k_1-wave (following wave)

$$\frac{R_{AW}}{\frac{1}{2}\rho g A^2}=\frac{1}{2}\left[-\frac{|H_D^+(k_2)|^2}{\sqrt{1-4\tau}}\left(1-\frac{k_2}{k_1}\right)+\frac{|H_D^-(k_3)|^2}{\sqrt{1+4\tau}}\left(1+\frac{k_3}{k_1}\right)\right.$$

$$\left.-\frac{|H_D^-(k_4)|^2}{\sqrt{1+4\tau}}\left(1+\frac{k_4}{k_1}\right)\right] \tag{51}$$

4) for incoming k_3-wave (following wave)

$$\frac{R_{AW}}{\frac{1}{2}\rho g A^2}=\frac{1}{2}\left[\frac{|H_D^+(k_1)|^2}{\sqrt{1-4\tau}}\left(1+\frac{k_1}{k_3}\right)+\frac{|H_D^+(k_2)|^2}{\sqrt{1-4\tau}}\left(1+\frac{k_2}{k_3}\right)\right.$$

$$\left.+\frac{|H_D^-(k_4)|^2}{\sqrt{1+4\tau}}\left(1-\frac{k_4}{k_3}\right)\right] \tag{52}$$

For a restrained circular cylinder, Grue & Palm proved that when the k_1-wave or the k_2-wave is incident upon the body, both k_3- and k_4-waves are not generated. Conversely for the case of incoming k_3- or k_4-wave, both k_1- and k_2-waves are not generated. With these characteristics, above equations (49)—(52) reduce to Grue & Palm's formulae. When the effects of body motions are taken into account, the motion-free Kochin function $H_F^{\pm}(k)$, defined by Eq. (23), must be substituted in place of the diffraction-problem Kochin function $H_D^{\pm}(k)$.

6. Numerical Results and Discussion

In practical calculations, the estimations of m-vector and hence of forward-speed potentials $\hat{\varphi}_j$ may be of principal complication. The calculation of m_j requires a solution for the steady perturbation potential φ_s, which satisfies the linearized free-surface condition (8) with $\omega=0$, the body boundary condition, and the radiation condition at infinity. In general, even if such a solution is numerically obtained, since numerical differentiations are required in twice for the evaluation of m_j, it may not be easy to keep sufficient accuracy. In order to investigate the m-vector contributions to the unsteady hydrodynamic forces without such a difficulty, we use the first-order approximation for φ_s: the infinite-fluid solution valid for a "deeply" submerged body. As well known, an analytical solution of φ_s for a circular cylinder is obtained. After a substitution of it into the definition of m-vector and a straightforward reduction, the m-vector can be obtained with the results

$$m_1=2\cos 2\theta\ ,\quad m_2=2\sin 2\theta\ . \tag{53}$$

These approximations of m-vector were used throughout the calculations presented in this paper.

The integral equation (11) was numerically solved in the following manner.

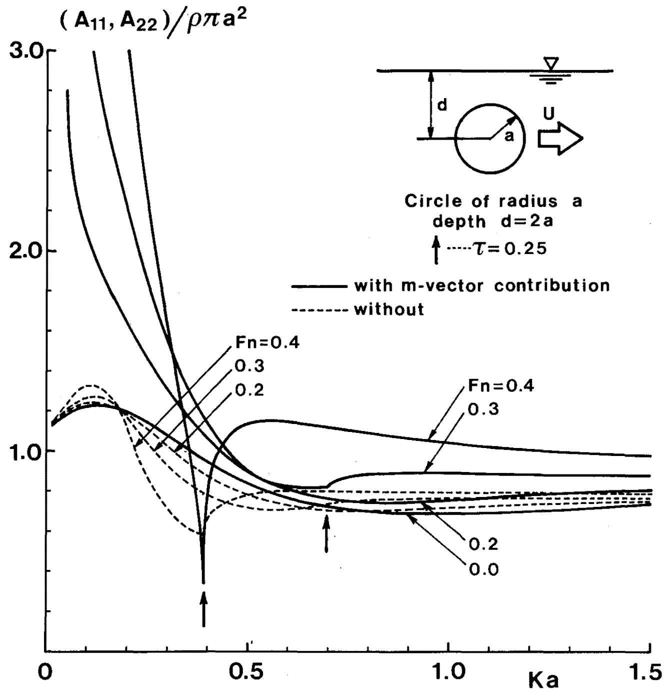

Fig. 3 Added-mass coefficient of circular cylinder for surge and heave motions.

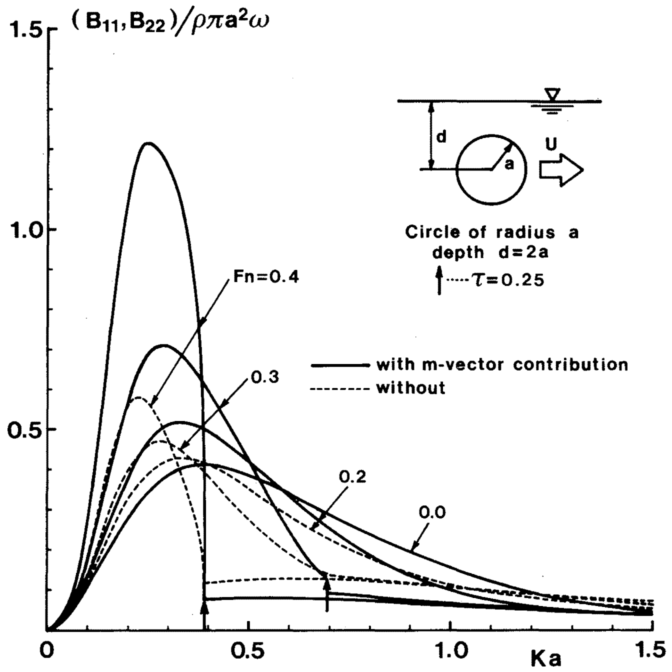

Fig. 4 Damping force coefficient of circular cylinder for surge and heave motions.

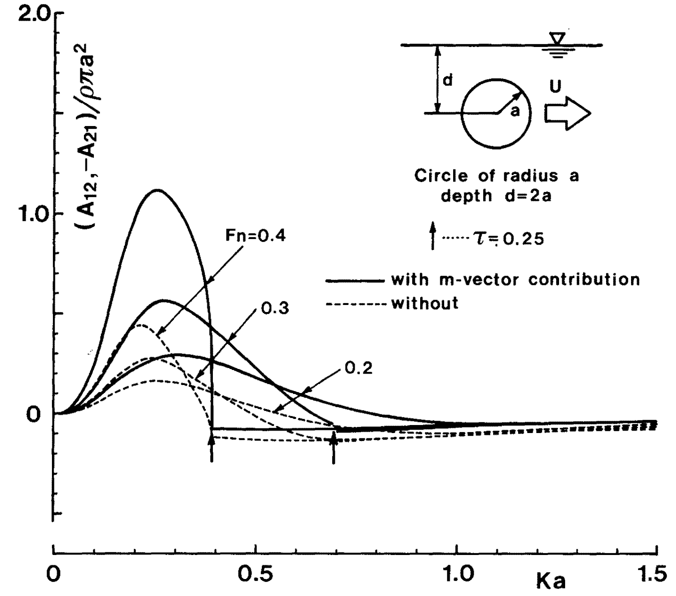

Fig. 5 Added-mass cross-coupling coefficients between surge and heave.

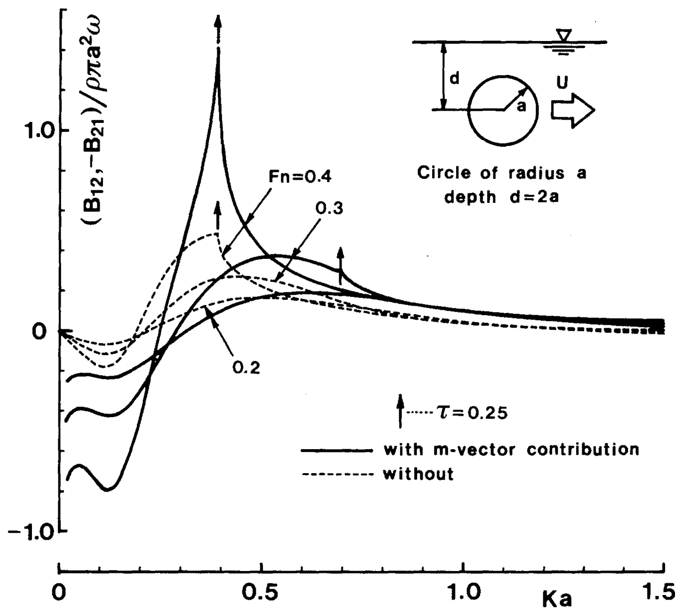

Fig. 6 Damping cross-coupling coefficients between surge and heave.

The body surface is discretized with N elements and the velocity potential $\phi(x, y)$ is assumed constant on each element. With the fact that ϕ is a complex quantity, a set of simultaneous equations with $2N$ unknowns are obtained; this was solved by the direct matrix-inversion method. To keep sufficient accuracy, the logarithmic term in the Green function was analytically integrated over the small individual element. The numerical accuracy was checked by the energy relation relating to the damping force for the radiation problem, and by the Haskind-Newman relation for the diffraction problem. With N set equal to 60, these relations were found to be satisfied with errors less than 0.5%.

The numerical results of the added-mass and damping coefficients are shown in Figs. 3—6 for a circular cylinder with its center placed at depth equal to twice the radius ($d/a = 2.0$). To investigate the forward-speed effects, calculations were performed for Froude numbers 0.0, 0.2, 0.3 and 0.4, and for respective Froude numbers, two kinds of numerical results are presented: one including the m-vector contributions (indicated by solid lines) and the other ignoring the m-vector throughout the calculations (indicated by dotted lines). The results of dotted lines are due to the first term on the right-hand side in Eqs. (38) and (39). It should be emphasized that the solid and dotted lines are respectively the results satisfying the energy relation with good accuracy. Comparison of solid and dotted lines reveals that the forward-speed effects on the body boundary condition (m-vector contributions) exert a large influence not to be neglected. In the frequency range higher than the critical frequency ($\tau = 1/4$), the effects of forward speed are relatively small. In our calculations, irrespective of the magnitude of forward speed, the added-mass and damping coefficients for surge motion are equal to the corresponding ones for heave motion; this is different from Grue's results[8] and is possibly due to the approximations of m-vector given by Eq. (53). The cross-coupling coefficients between surge and heave, shown in Figs. 5 and 6, were numerically confirmed to satisfy the Timman-Newman symmetry relations[9] with quite small errors.

The wave-exciting forces for head and following waves are presented in Fig. 7 and Fig. 8, respectively. Both the amplitude and the phase are shown. We note that the amplitudes are equal but the phase difference of 90 degrees exists between surge and heave exciting forces. As seen from Fig. 7, the forward-speed effects in head waves are small, but the maximum gradually decreases with increasing Froude number. On the other hand, in following waves (see Fig. 8), the amplitude of exciting force increases in the low frequency range as the Froude number increases. However as the frequency approaches the critical frequency where the velocity of the body is equal to the group velocity of incident wave, the amplitude becomes small and vanishes at the critical frequency. Similarly the phase difference changes greatly near the critical frequency. In Figs. 7 and 8, also included are the results of the approximate analysis with a simple conclusion that the exciting forces are independent of the forward speed. This approximate analysis, which is presented in Appendix B,

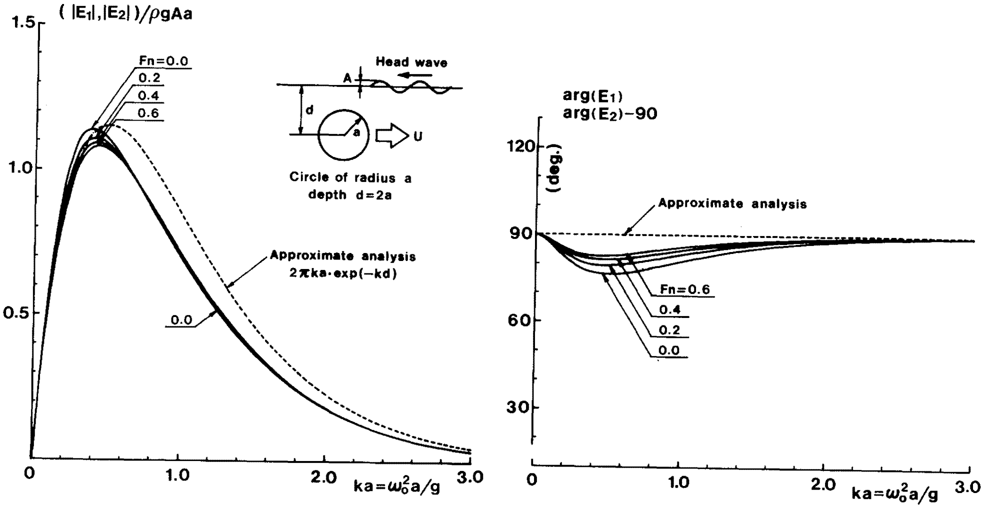

Fig. 7 Wave-exciting force for surge and heave motions of circular cylinder in head waves, amplitude (left) and phase difference (right).

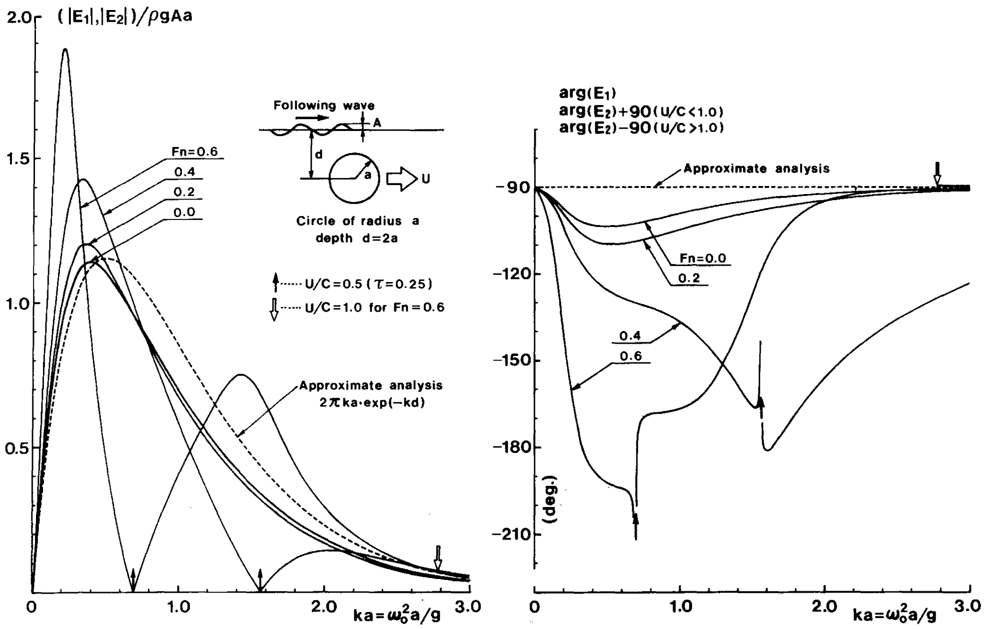

Fig. 8 Wave-exciting force for surge and heave motions of circular cylinder in following waves, amplitude (left) and phase difference (right).

is an extention of Ogilvie's approximate method[12] for zero-speed problem to the forward-speed case. In this analysis, the free surface condition is violated. Therefore the discrepancies between exact and approximate results imply that the forward-speed effects on the free-surface condition are large, especially in following waves.

Having obtained the first-order hydrodynamic forces, we can calculate the motions of a circular cylinder responding to those forces. The cylinder is assumed to have the same density as the fluid and to be stable. Then, with the linear assumption, the following equations can be used to describe the coupled motions between surge and heave:

$$\sum_{j=1}^{2}\left[-\omega^2(m\delta_{ij}+A_{ij})+i\omega B_{ij}\right]\xi_j = E_i \quad (i=1,2)\ , \tag{54}$$

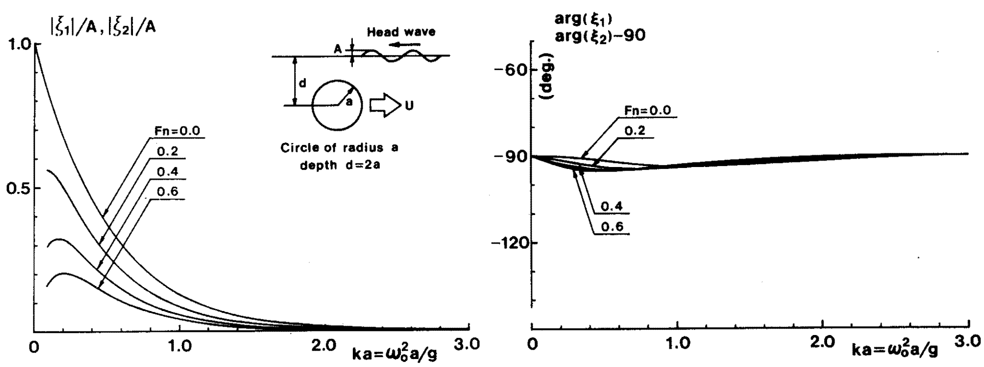

Fig. 9 Surge and heave motions of circular cylinder in head waves, amplitude (left) and phase difference (right).

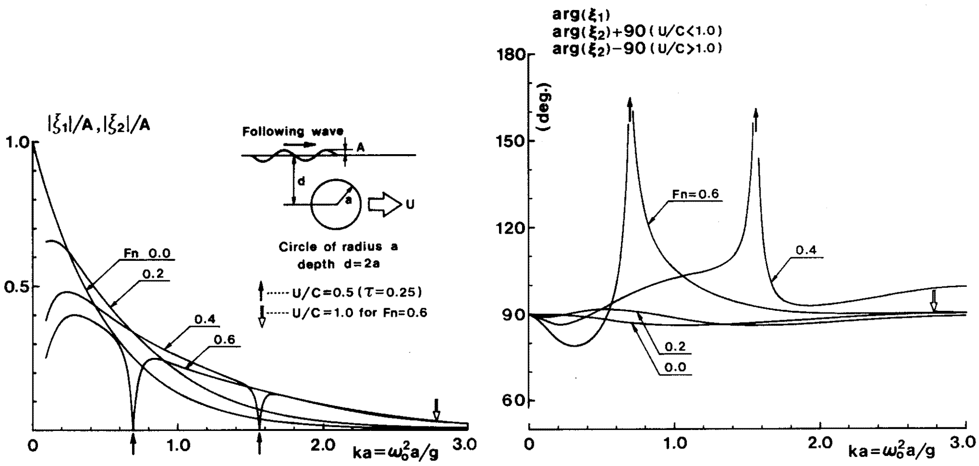

Fig. 10 Surge and heave motions of circular cylinder in following waves, amplitude (left) and phase difference (right).

where m denotes the body mass and δ_{ij} the Kroenecker delta function.

The absolute value and phase of the "complex" amplitude of motion ξ_j are shown in Fig. 9 for head waves and in Fig. 10 for following waves. As is the same as the first-order hydrodynamic forces, the amplitudes of surge and heave motions are identical. It is seen from Figs. 9 and 10 that in head waves the forward speed affects the body motion to reduce its amplitude, whereas in following waves, due to the effects of forward speed the amplitude becomes large compared to the zero-speed case except in the very low frequency-range.

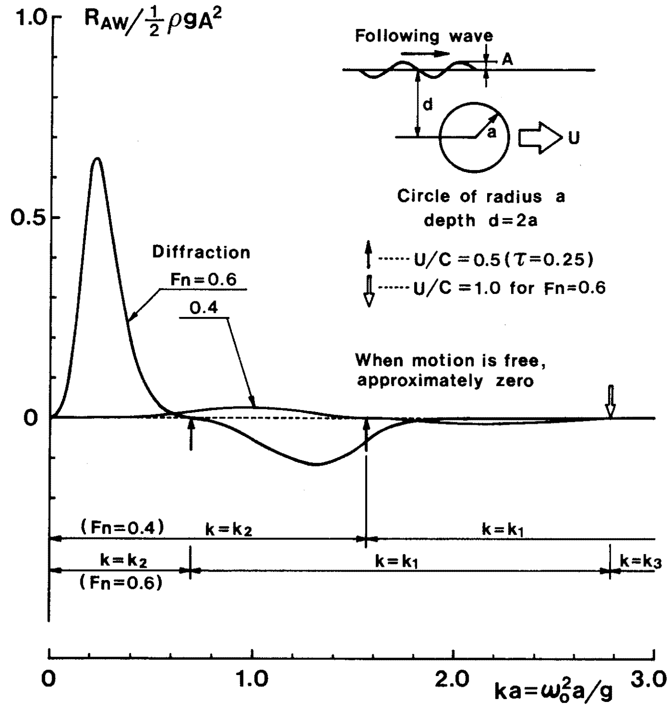

Fig. 11 Added resistance of circular cylinder in following waves.

Fig. 11 shows the added resistance of a circular cylinder restrained in its steady-state equilibrium position in following waves. The added resistance in head waves turned out to be approximately zero. (Thus the graph is not shown.) The reason for this is as follows. As proved by Grue & Palm[7], both k_1- and k_2-waves are not generated for the incoming k_4-wave. Thus, from Eq. (49), the added resistance in head waves results from only k_3-wave contribution; this is quite small, since the amplitude of k_3-wave is almost zero. In relation to the following-wave problem, Grue & Palm showed that both k_3- and k_4-waves are not generated when the incident wave is k_1- or k_2-wave. From Eqs. (50) and (51) it can be understood that the added resistance is positive for the incoming

k_2-wave, whereas it is negative for the incoming k_1-wave. These analytical properties can be confirmed by the numerical results presented in Fig. 11. With the fact that the k_1-wave originates from the steady-translation problem, it is expected that the added resistance for incoming k_2-wave increases with the increasing Froude number ; this may be also confirmed by Fig. 11. We emphasize that these interesting results on the added resistance may not be true for the body of general shape.

If the body is allowed to respond to the first-order wave-exciting forces, all four waves of different wavenumbers k_j ($j = 1, 2, 3, 4$) will contribute to the added resistance. Using the numerical results of the complex amplitude of motion, we calculated the added resistance from Eqs. (49)—(52) with $H_D^{\pm}(k_j)$ replaced by $H_F^{\pm}(k_j)$, defined by Eq. (23). From numerical computations we found that there is no added resistance when the motions of a circular cylinder are allowed. As for the case of zero forward speed, Ogilvie[12] showed analytically that no horizontal steady force acts on the circular cylinder which is free to respond to incident waves. Thus, the result numerically found in this paper may be regarded as a generalization of Ogilvie's result to the forward-speed case.

7. Concluding Remarks

We showed numerical results of hydrodynamic forces acting on a two-dimensional circular cylinder moving with forward velocity and oscillating under the effects of incident waves. Then we investigated the forward-speed effects on hydrodynamic forces.

The effects of forward speed on the body boundary condition, resulting from the interactions between steady and oscillatory flow fields, turned out to contribute to the hydrodynamic forces with considerable magnitude.

Due to the effects of free-surface boundary condition, four waves of different wavenumbers are generated. These four waves affect individually the hydrodynamic forces on a body to varying degrees, depending on the magnitude of forward speed and frequency of oscillation of the body. Such complicated effects were clarified to some extent by the numerical calculations presented here. We believe that the present study will provide some information to the three-dimensional problem with forward speed.

References

1) Ogilvie, T. F. and Tuck, E. O. : *A rational strip theory for ship motions,* Dept. Nav. Arch. Mar. Eng., Univ. Michigan, Rep. No. 13, (1969) pp. 1-92.

2) Faltinsen, O. : *A numerical evaluation of the Ogilvie-Tuck formulas for added mass and damping coefficients,* J. Ship Res., Vol. 18, (1974) pp. 221-283.

3) Chapman, R. B. : *Numerical solution for hydrodynamic forces on a surface-piercing plate oscillating in yaw and sway,* 1st Int. Conf. on Numerical ship Hydrodynamics, Gaithersburg, Maryland, (1975) pp. 333-350.

4) Chang, M. S : *Computations of three-dimensional ship motions with forward speed,* 2nd

Int. Conf. on Numerical Ship Hydrodynamics, Univ. California, Berkeley, (1977) pp. 124-135.

5) Kobayashi, M.: *On the hydrodynamic forces and moments acting on a three dimensional body with a constant forward speed (in Japanese)*, J. Soc. Nav. Arch. Japan, Vol. 150, (1981) pp. 175-189.

6) Ursell, F.: *Mathematical notes on the two-dimensional Kelvin-Neumann problem of ship hydrodynamics,* 13th Symp. on Naval Hydrodynamics, Tokyo, (1980).

7) Grue, J. and Palm, E.: *Wave radiation and wave diffraction from a submerged body in a uniform current,* J. Fluid. Mech., Vol. 151, (1985) pp. 257-278.

8) Grue, J.: *Time-periodic wave loading on a submerged circular cylinder in a current,* J. Ship Res., Vol. 30, No. 3, (1986) pp. 153-158.

9) Timman, R. and Newman, J. N.: *The coupled damping coefficients of symmetric ships,* J. Ship Res., Vol. 5, No. 4, (1962) pp. 34-55.

10) Newman, J. N.: *The exciting forces on a moving body in waves,* J. Ship Res., Vol. 9, (1965) pp. 190-199.

11) Maruo, H.: *Wave resistance of a ship in regular head seas,* Bulletin of the Faculty of Eng., Yokohama National Univ., Vol. 9, (1960) pp. 73-91.

12) Ogilvie, T. F.: *First-and second-order forces on a cylinder submerged under a free surface,* J. Fluid Mech., Vol. 16, (1963) pp. 451-472.

13) Milne-Thomson, L. M.: *Theoretical Hydrodynamics,* 4th edition, MacMillan, New York, (1960).

Appendix A
Derivation of equations for damping force and added resistance

Deriving the two-dimensional results from the corresponding three-dimensional ones may be helpful for a better understanding of the relationships between two- and three-dimensional problems.

The three-dimensional result for the damping coefficient, which can be obtained by applying the principle of energy conservation[11], is written as follows

$$B = \frac{\rho\omega}{4\pi}\left[\int_{-\pi/2}^{-\alpha_0} + \int_{\alpha_0}^{\pi/2} - \int_{\pi/2}^{3\pi/2}\right]\frac{|H(\kappa_1, \alpha)|^2}{\sqrt{1-4\tau\cos\alpha}}\kappa_1 d\alpha$$
$$+\frac{\rho\omega}{4\pi}\int_{\alpha_0}^{2\pi-\alpha_0}\frac{|H(\kappa_2, \alpha)|^2}{\sqrt{1-4\tau\cos\alpha}}\kappa_2 d\alpha\ , \tag{A1}$$

where

$$\left.\begin{matrix}\kappa_1\\ \kappa_2\end{matrix}\right\} = \frac{K_0}{2\cos^2\alpha}\left[1-2\tau\cos\alpha \pm \sqrt{1-4\tau\cos\alpha}\right]\ , \tag{A2}$$

$$H(\kappa_j, \alpha) = \iint_{S_H}\sigma(\xi, \eta, \zeta)e^{-\kappa_j\zeta} + e^{i\kappa_j(\xi\cos\alpha+\eta\sin\alpha)}dS\ , \tag{A3}$$

$$\alpha_0 = \begin{cases} 0 & \text{for } \tau < 1/4 \\ \cos^{-1}(1/4\tau) & \text{for } \tau > 1/4 \end{cases} \tag{A4}$$

Here α is physically the direction in which elementary plane waves propagate, and σ denotes the source strength distributed on the three-dimensional body surface.

In the two-dimensional case, since the source distributions are confined to the ξ-ζ plane, we write as

$$\sigma(\xi, \eta, \zeta) = \sigma(\xi, 0, \zeta) \equiv \sigma(\xi, \zeta) . \tag{A5}$$

Substituting this in Eq. (A3), we get

$$\begin{aligned} H(\kappa_j, \alpha) &= \int_{S_H} \sigma(\xi, \zeta) e^{-\kappa_j\zeta + i\kappa_j\xi\cos\alpha} dl(\xi, \eta)\cdot 2\pi\delta(\kappa_j \sin\alpha) \\ &\equiv H_{2D}(\kappa_j, \alpha) 2\pi\delta(\kappa_j \sin\alpha) , \end{aligned} \tag{A6}$$

where $\delta(x)$ is Dirac's delta function defined by

$$\delta(x) = \frac{1}{2\pi}\int_{-\infty}^{\infty} e^{ix\eta} d\eta , \tag{A7}$$

and this function has the following property

$$\delta(kx) = \frac{1}{|k|}\delta(x) \tag{A8}$$

From these equations, we notice that when deriving the corresponding two-dimensional result from Eq. (A1), the following relation must be substituted:

$$\frac{\kappa_j}{2\pi}|H(\kappa_j, \alpha)|^2 \to |H_{2D}(\kappa_j, \alpha)|^2\delta(\sin\alpha) \tag{A9}$$

The relations of the wavenumbers $\kappa_1(\alpha)$, $\kappa_2(\alpha)$ to the two-dimensional wavenumbers k_j $(j = 1, 2, 3, 4)$ are found to be

$$\left.\begin{aligned} k_1 &= \kappa_1(0) , \quad k_2 = \kappa_2(0) , \\ k_3 &= \kappa_1(\pi) , \quad k_4 = \kappa_2(\pi) . \end{aligned}\right\} \tag{A10}$$

Futhermore, comparison of $H_{2D}(\kappa_j, \alpha)$ in Eq. (A6) with the two-dimensional Kochin function $H^{\pm}(k_j)$ defined by Eq. (22) gives the relations

$$\begin{aligned} H_{2D}(\kappa_j(0), 0) &= H^{+}(k_j) , \\ H_{2D}(\kappa_j(\pi), \pi) &= H^{-}(k_i) . \end{aligned} \quad \text{for} \begin{pmatrix} j = 1, 2 \\ i = 3, 4 \end{pmatrix} \tag{A11}$$

With these relations taken into account, the two-dimensional result will be readily obtained from Eq. (A1). The result obtained in this manner certainly agrees with Eq. (40).

With the same argument, the equation for the two-dimensional added resistance can be derived from well-known three-dimensional Maruo's formula [11], given by

$$\frac{R_{AW}}{\frac{1}{2}\rho g A^2} = \frac{1}{4\pi K}\left[\int_{-\pi/2}^{-\alpha_0} + \int_{\alpha_0}^{\pi/2} - \int_{\pi/2}^{3\pi/2}\right]\cdot|H(\kappa_1, \alpha)|^2 \frac{\kappa_1(\kappa_1\cos\alpha - K\cos\chi)}{\sqrt{1-4\tau\cos\alpha}} d\alpha$$

$$+\frac{1}{4\pi K}\int_{\alpha_0}^{2\pi-\alpha_0}|H(\kappa_2,\alpha)|^2\frac{\kappa_2(\kappa_2\cos\alpha-K\cos\chi)}{\sqrt{1-4\tau\cos\alpha}}d\alpha\ , \qquad \text{(A12)}$$

where

$$K=\frac{K_0}{2\cos^2\chi}\left[1-2\tau\cos\chi\pm\sqrt{1-4\tau\cos\chi}\right]\ . \qquad \text{(A13)}$$

Since χ denotes the direction of the plane progressive incident wave, χ is put to be 0 or π for the two-dimensional case. Then the wavenumber K given by Eq. (A13) takes four values corresponding to the four wavenumbers k_1, k_2, k_3, k_4, defined in the two-dimensional problem. Therefore applying to Eq. (A12) the same limiting operation as that in deriving the damping force, we can obtain the general expression for the two-dimensional added resistance, which is subdivided into four cases according to the wavenumbers of the incident wave (see Eqs. (49)-(52)).

Appendix B
Approximate analysis for wave-exciting force

We extend Ogilvie's approximate analysis[12] for the zero-speed problem to the case of nonzero speed.

First let us consider the case of head waves. The complex potential of the incident wave superposed on a uniform flow is written in the form

$$f_0(z,t)=-Uz+\frac{gA}{i\omega_0}e^{i(kz+\omega t)}\ , \qquad \text{(B1)}$$

where

$$z=\zeta+id\ ,\quad \zeta=re^{i\theta}\ . \qquad \text{(B2)}$$

If there were no free surface present, Milne-Thomson's circle theorem[13] could be used to find the change caused by a restrained circular cylinder. Applying this theorem, the total complex potential is given by

$$f(z,t)=-U\left(z+\frac{a^2}{z-id}\right)$$
$$+\frac{gA}{i\omega_0}\left\{e^{i(kz+\omega t)}-e^{-kd}e^{-i\left(\frac{ka^2}{z-id}+\omega t\right)}\right\}\ . \qquad \text{(B3)}$$

The pressure on the body surface can be calculated in terms of Bernoulli's equation of the form

$$-\frac{p}{\rho}=\Phi_t+\frac{1}{2}(\Phi_x^2+\Phi_y^2)$$
$$=Re\left\{\frac{df}{dt}+\frac{1}{2}\frac{df}{dz}\cdot\overline{\frac{df}{dz}}\right\}\ . \qquad \text{(B4)}$$

After substituting the derivations of Eq. (B3) into Eq. (B4) and retaining only terms that are sinusoidal in time with the frequency ω, we get

$$-\frac{p}{\rho} = 2\omega_0 A e^{-kd} Re\left[\left(\frac{\omega_0}{k} + Ue^{i2\theta}\right) \exp(ikae^{i\theta}) e^{i\omega t}\right] . \tag{B5}$$

Where the relation $\omega = \omega_0 + kU$ was taken into account. The first-order exciting forces are obtained by integrating this pressure over the body surface. That is,

$$X - iY = -\int_0^{2\pi} pe^{-i\theta} ad\theta . \tag{B6}$$

Substituting Eq. (B5) in Eq. (B6) and taking account of the relations

$$\left.\begin{aligned} \exp(ikae^{i\theta}) &= \sum_{m=0}^{\infty} \frac{(ika)^m}{m!} e^{im\theta} \\ \text{and} \qquad \int_0^{2\pi} e^{in\theta} d\theta &= 2\pi\delta_{n,0} , \end{aligned}\right\} \tag{B7}$$

we get the final expression for the first-order exciting forces in the form

$$\frac{X - iY}{\rho g A a} = i2\pi kae^{-kd} e^{i\omega t} . \tag{B8}$$

This result is independent of the forward speed and thus the same as that for zero-speed problem shown by Ogilvie. Since Eq. (B3) is correct for sufficiently large depth ratio d/a, Eq. (B8) is expected to give reasonable predictions for a deeply submerged circular cylinder.

The approximate analysis for the case of following waves can be performed in the same manner. Starting with the complex potential for the following wave in a uniform flow, given by

$$f_0(z, t) = -Uz - \frac{gA}{i\omega_0} e^{i(kz - \omega t)} , \tag{B9}$$

the final result corresponding to Eq. (B8) will be obtained in the following form

$$\frac{X + iY}{\rho g A a} = -i2\pi kae^{-kd} e^{i\omega t} . \tag{B10}$$

This formula is also independent of the forward speed. But, as was shown by exact numerical calculations, the exciting forces in following waves have strong dependence on the forward speed; this is apparently due to the effects of forward speed on the free-surface condition, since the approximate analysis presented here does not satisfy the exact free-surface condition.

(Received July 15, 1987)